A TRANSIENT MULTIPHYSICS THERMAL/CFD SIMULATION ANALYSIS OF A MOLTEN REGOLITH ELECTROLYSIS REACTOR WITHIN A THERMAL VACUUM CHAMBER

Laurent Sibille
ASTRION
Exploration Systems, Swamp Works
NASA Kennedy Space Center, FL

William Dziedzic
NASA Kennedy Space Center

Evan A Bell
NASA Kennedy Space Center

ABSTRACT

An electrochemical technique, called Molten Regolith Electrolysis (MRE) performs the direct electrolysis of molten lunar regolith to obtain gaseous oxygen and liquid metal mixtures separately. In a MRE process, granular lunar regolith is placed into a reactor and heated to a molten state. Kennedy Space Center (KSC) is assisting Lunar Resources, Inc. (LR) in the design of a full reactor test under vacuum conditions to provide requirements for safe operations during a fully integrated test campaign. The reactor will be tested at the KSC facility and will meet NASA safety and engineering requirements during the development. A transient multiphysics thermal/CFD analysis of a MRE reactor is developed to simulate the melting of the lunar regolith to support reactor design development and protect the walls of the thermal vacuum chamber.

The reactor test is designed to demonstrate the production of a minimum of 10 wt.% of the total oxygen from the regolith mass that has been heated to a temperature of 1600°C. The reactor test is also designed to enable the selection or permutations of subsystems to be tested such as those for molten material handling, regolith feed, and regolith melting.

The transient thermal/CFD analysis of the reactor and thermal vacuum chamber uses a commercial software package called COMSOL Multiphysics[1]. The multiphysics analysis includes heat transfer in solids and fluid analysis. Radiation includes both surface-to-surface radiation and radiation in a participating media. A scaled test was used to determine the time-dependent heating power conditions for the analysis. The results of the simulation will include a time history plot of temperatures on the internal/external thermal vacuum chamber walls. The analysis will be used during test to compare measured temperatures with simulated values to monitor the progress of the test and aid in identifying any non-nominal conditions.

NOMENCLATURE, ACRONYMS, ABBREVIATIONS

ASSIST	Atmospherically Sealed Simulator for In-Situ System Testing
CFD	Computational Fluid Dynamics
KSC	Kennedy Space Center
MRE	Molten Regolith Electrolysis
VMOMS	Volatile Monitoring and Oxygen Measurement System
LR	Lunar Resources, Inc.

INTRODUCTION

Molten Regolith Electrolysis (MRE) is a technique for producing gaseous oxygen and various metals from unprocessed regolith (soil) in a single-step process reactor and can be operated at various planetary destinations including the moon and Mars. It consists in melting a mass of regolith and performing direct electrolysis of the ionic electrolyte at high temperature to form gaseous oxygen at the anode and collect alloying metals in liquid state at the cathode. The electrolysis process also provides internal heating of the melt mass by Joule-heating effect. The technology behind an MRE reactor has been under development for several years and is currently positioned to begin larger scale testing of a reactor. The current MRE project led by NASA KSC will demonstrate and test a sub-scale and fully integrated reactor developed in collaboration with Lunar Resources, Inc. a commercial partner. The results of the reactor test, plus lessons learned from executing this project, will help influence NASA's approach for investment and maturation of the MRE technology and better position the technology to be flown on a lunar demonstration mission.

The MRE test reactor is designed and built by LR to perform regolith melting, electrolyze the melt to produce oxygen, and perform a one-time addition of unprocessed regolith to the melt pool. The system has interface points for oxygen collection, liquid metals extraction and molten regolith removal. The reactor design also accommodates various regolith heating options (e.g., resistive to form the molten mass prior to starting the electrolysis to enable flight forward technology tests by KSC.

The objective of the MRE project is to perform an integrated test of the MRE reactor under a vacuum environment (also simulating the black body absorption of the reactor's radiative heat by cooling the ASSIST to near-room temp (relative to the reactor)) in the Atmospherically Sealed Simulator for In-Situ System Testing (ASSIST) vacuum chamber at KSC's Swamp Works

laboratory. The test reactor will electrolyze a single batch of regolith while under vacuum to extract a targeted 10 wt.% of the regolith mass in the form of oxygen at the anode and a corresponding mass of metal alloys at the cathode.

The reactor will be tested at the NASA facility and will meet NASA safety and engineering requirements during development. The work presented in this paper focuses on the thermal/CFD modeling and transient simulation of the reactor and the vacuum chamber that are performed to provide design guidance and ensure adequate protection of the chamber. The illustrations omit detailed views of the reactor design to protect proprietary information.

OBJECTIVES AND SYSTEM MODELS

Objectives

The modeling and simulation task is aimed at providing a comprehensive description of the thermal environment of the combined system of the MRE reactor and the ASSIST chamber during selected phases of operations to assess the feasibility of conducting the test while ensuring that both the reactor and its subsystems and the ASSIST chamber remain within safe limits thermally. Pursuant of this goal, the effort was structured to achieve the following objectives:

- Build a medium-fidelity model of a MRE reactor in the ASSIST thermal vacuum chamber for thermal simulation in COMSOL.
- Perform simulations of the transient thermal behavior of the reactor operating under vacuum conditions in the ASSIST for different analysis cases.
- Validate the thermal model using data from subscale heating subsystem tests performed in the ASSIST at KSC.
- Characterize the thermal environment of the ASSIST during expected reactor operations and identify protection options to maintain the temperatures of the internal walls of the chamber to below 150℃ per the design limits of the ASSIST chamber.

System models and assumptions

Reactor Model

The reactor is modeled in 3 dimensions with materials properties in agreement with the as-built reactor specifications. The gaseous atmosphere inside the reactor is modeled as originating from the anode surface and exiting at a targeted pressure to the VMOMS system as convection and heat loss from out-flow of gas is simulated. The reactor includes the following components and subsystems that are modeled using as-built CAD files:

1. Reactor structure
   a. Metal shell with ports for electrical input, sensors, material handling subsystems, frame that rests on the brick pan, etc.

b. Reactor insulation subsystem
2. Regolith heating subsystem
3. Anode and cathode subsystems
4. Regolith addition subsystem
5. Reactor control system
6. Oxygen and Volatile measurement subsystem (VMOMS)

Reactor Heating Subsystem Model

The internal structure of the heating system is not modeled to minimize meshing density while the heating model is focused on describing the heat transfer into the regolith and the surrounding reactor. The interface between the heating system and the regolith is modeled as a refractory ceramic surface through which radiative and conductive heat transfer occurs. Heat conduction is modeled from the hot zone to the rest of the heating system, and the reactor.

Regolith Mass Model

The properties of the lunar regolith assigned as a function of temperature; the properties of the regolith simulant selected for the test are used when they are known experimentally. In the absence of the latter, published values of properties of highland regolith are used. Melt properties are assigned according to the same methodology as for regolith. The circulation of electric current through the melt and the resulting Joule-heating effects during electrolysis is not modeled but will be part of future work. Surfaces of the anode and cathode within the melt mass are assigned a constant temperature of 1600℃ to simulate thermal equilibrium at the targeted operational temperature during the electrolysis phase of the reactor that generates Joule heating.

ASSIST Chamber Model

The ASSIST chamber model is a manufacturer's CAD file without the flanges and ports to simplify meshing for the intended simulations. Water-cooled side walls are modeled by a heat extraction rate. No atmosphere is assigned inside ASSIST (perfect vacuum). Power cables, O_2 line and coolant lines are included to aid in finding their optimal placement with respect to thermal environment. The expected heat extraction rate to the O_2 heat exchanger is modeled to verify expected temperature of outflowing O_2 to VMOMS.

Figure 1 shows the test set up of the chamber with supporting equipment to ensure thermal protection.

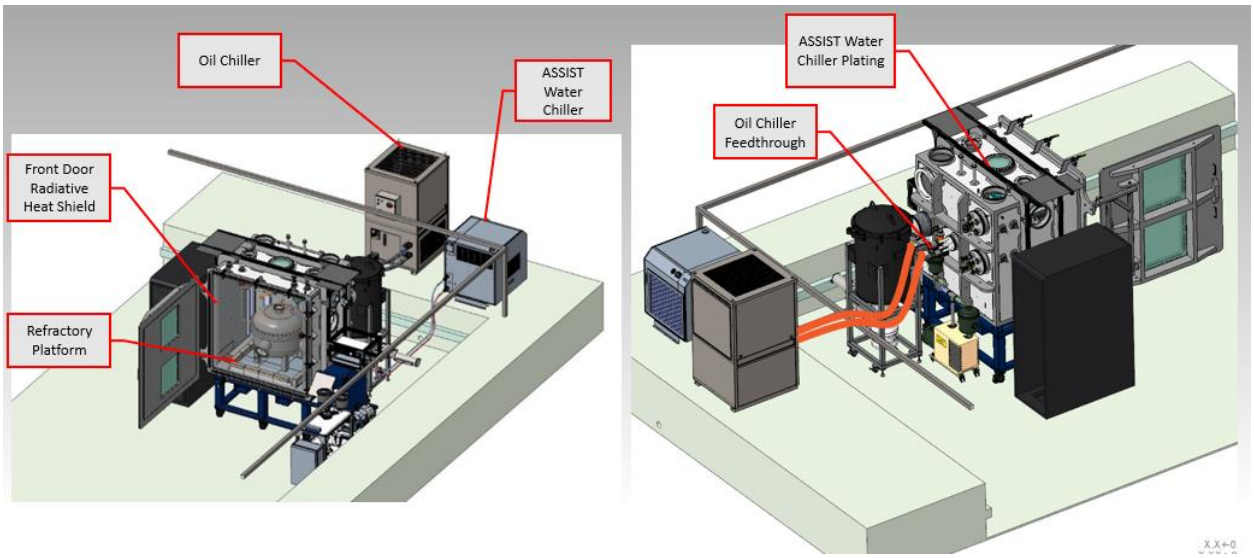

Figure 1. ASSIST thermal protection systems and reactor.

The ASSIST model includes the chamber walls, two borosilicate glass windows in the door, and the chamber supporting pillars as shown in Figure 2. The ceiling and side walls are water cooled with a recirculating chiller set at 20°C. The door is not water cooled and it and the windows require protection from radiative heat transfer from the reactor. A radiative heat shield installed a few centimeters from the door consists of an aluminum plate fastened to water-cooled side walls to cool the plate by conduction.

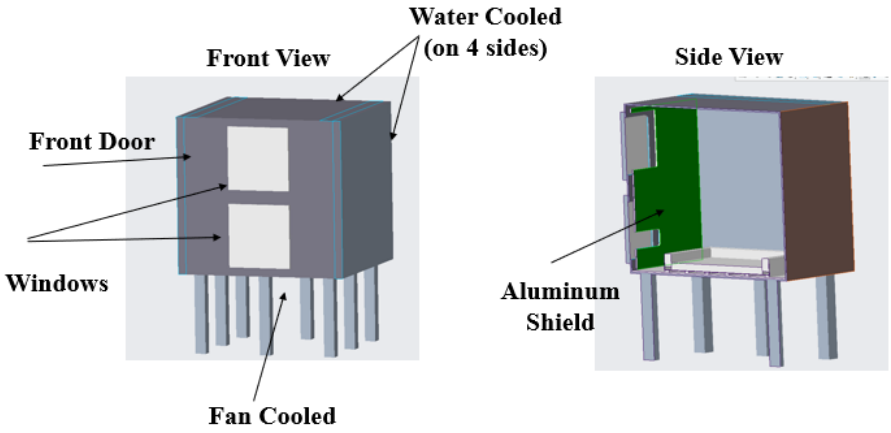

Figure 2. ASSIST chamber model with front door windows (left). An aluminum plate (right, in green) fastened to the water-cooled walls serves as a radiative heat shield to protect door and windows.

Figure 3 displays the modeled elements that comprise the thermal protection of the floor directly underneath the reactor. A 304 stainless steel stand engineered to support the MRE reactor is placed

on a refractory platform made of an assembly of high temperature refractory bricks layered on a 304 stainless steel platform. An aluminosilicate blanket adds protection below the platform and to wires and fluid lines around it. A fan provides convective cooling underneath the ASSIST floor. A corner mirror allows viewing of reactor areas hidden from the door windows.

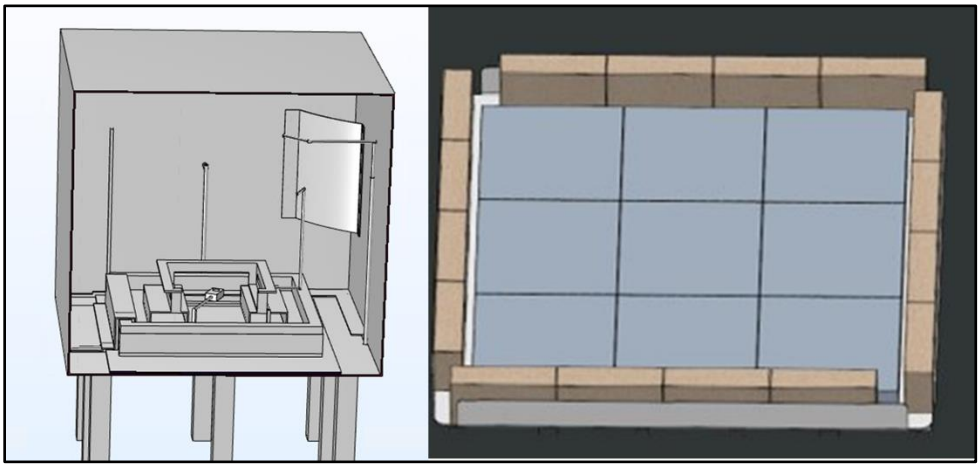

Figure 3. Thermal protection elements for the ASSIST chamber floor. The refractory platform (right) supports a steel stand on which the reactor is emplaced (left).

ANALYSIS METHODOLOGY

The transient thermal/CFD analysis of the reactor and thermal vacuum chamber uses a commercial software package called COMSOL Multiphysics. The multiphysics analysis includes heat transfer in solids and fluid analysis. Radiative heat transfer is included as both surface-to-surface radiation and radiation in a participating media represented by the regolith region. Heat input into the system was modeled using experimental data acquired during subscale regolith melting tests using the same heating subsystem to determine the time-dependent heating power conditions for the analysis. The results of the simulation include a time history plot of temperatures on the internal and external thermal vacuum chamber walls.

Approach

The COMSOL model does not include electrolysis and Joule-heating caused by the electrolytic current through the melt that heats the reactor internally. Consequently, the approach involves validating the heating model of the melt using thermal data collected during a separate subscale melt test in vacuum using the heating system. The validated model is then applied to simulate the reactor heating phase until a regolith melt mass is formed between the electrodes. The heating phase simulation is then followed by an electrolytic phase simulated thermally by a constant and uniform melt temperature selected as the operating temperature for each simulation. The heating system is assumed in a non-energized state during the electrolytic phase.

MRE Thermal Process Steps for Simulation

The Multiphysics simulation of the MRE reactor operations is designed to accept a range of values as user inputs for the subscale heating system power and duration, target temperatures for the melt, duration of the test at target temperature, and water and oxygen mass flow rate from the anode.

The work presented here is a representative example of many potential operational settings for an actual MRE reactor test with a target duration of 37.5 hours. The target melt temperatures listed below are selected based on the thermophysical properties of the regolith simulant CSM-LHT-1G selected for this test (see later section on regolith simulant properties). In this case, 1400°C represents the liquidus temperature at which all components of the regolith are molten. The simulation example is described below in two separate operations that are performed sequentially in COMSOL.

1. Heating Phase: The regolith is gradually heated to 1400°C via heating system over the course of 17.5 hours. The target temperature is selected to ensure the melt is fully formed and can pass electrical current for the subsequent electrolysis phase.
2. Electrolysis Phase: The electrodes are energized to pass current through the regolith melt pool for 20 hours. The electrical physics are not part of the simulation.
    - Regolith heating is turned off during the electrolysis phase.
    - Joule-heating of regolith by electrolytic current is assumed to sustain the melt mass temperature at 1600°C. In the simulation, the melt mass temperature is kept at this steady-state value.

The power curve used for the subscale heating system during the heating phase is shown below (Figure 4) and is used as input for the heating phase simulation. The scale of the heating system is proprietary and is not disclosed in this paper. The values in the figure are that of a subscale system to illustrate the heating rate only.

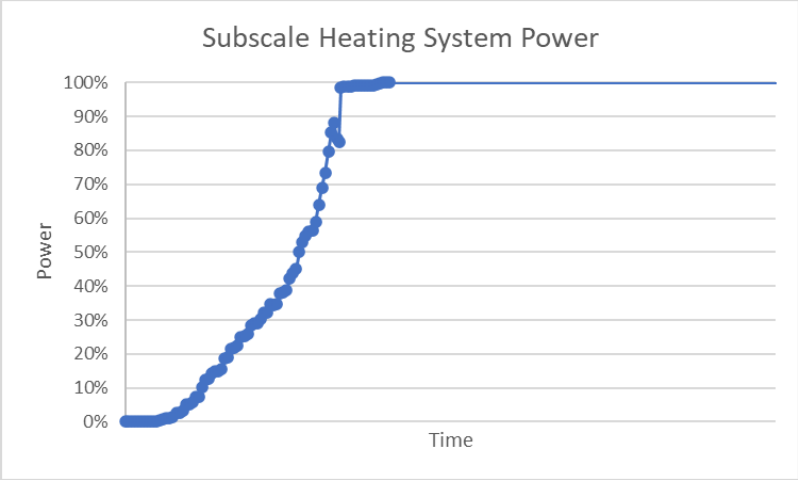

Figure 4. Subscale heating system power.

Materials and Thermophysical Properties

Selection of Lunar regolith simulant material

Samples of lunar regolith are not made available by NASA to perform experimental tests that would result in permanent alterations of the samples. Consequently, technology tests such as the one described in this work require the use of simulant materials of the regolith. These materials are typically sourced from terrestrial natural rock and mineral mixtures that approximate the most relevant characteristics of the targeted lunar material. Lunar regolith is formed by breakage and comminution of lunar rocks under the combined forces of meteoritic impacts and thermal cycling between day and night temperatures. This formation process produces a dry material typically described as a well-graded/poorly sorted, silty sand to sandy silt that corresponds to the Unified Soil Classification System categories “SW-SM” to “ML”. The median particle size is 40 to 130 μm, with an average of 70 μm. It is distributed ubiquitously over the entire Moon to a depth of several meters with consistent physical characteristics and with mineralogical variations that depend on the region or location of interest.

The lunar destinations currently targeted by NASA’s Artemis program are in the south polar regions where highlands mineralogy dominates. The selection of a suitable simulant material for the MRE process focused on a high weight percent of Anorthosite rock (with high anorthite content) and a high glass content (30-40 wt.%) of similar origin as the anorthosite to represent the chemical composition and the glass formed by meteoritic impact on the Moon. In addition, the selection included a desired iron content of ~ 5-7 wt.% of FeO and low levels of impurity to reduce safety risks from hazardous volatiles and reduce unwanted electrochemical effects.

The simulant selected for this work is CSM-LHT-1G produced from anorthosite and basalt that contains a high glass content to approximate the viscosity of polar lunar material as best as possible (**Table 1**).

Table 1. General mineralogy of CSM-LHT-1G selected as simulant of lunar polar material

Mineralogical composition	wt.%
Anorthosite (rock suite)	55.2
Basalt / norite	15.15
Basaltic glass	11.7
Glass (basaltic, and synthetic)	15.2

Regolith Thermal Conductivity

The thermal conductivity of the granular regolith simulant as a function of temperature was modeled using the "Continuous fit" curve of data (shown in Figure 5). This data was collected under vacuum for several simulants and Apollo samples published by Schreiner et al.[2] The data for molten phase is modeled based on slag compositions.

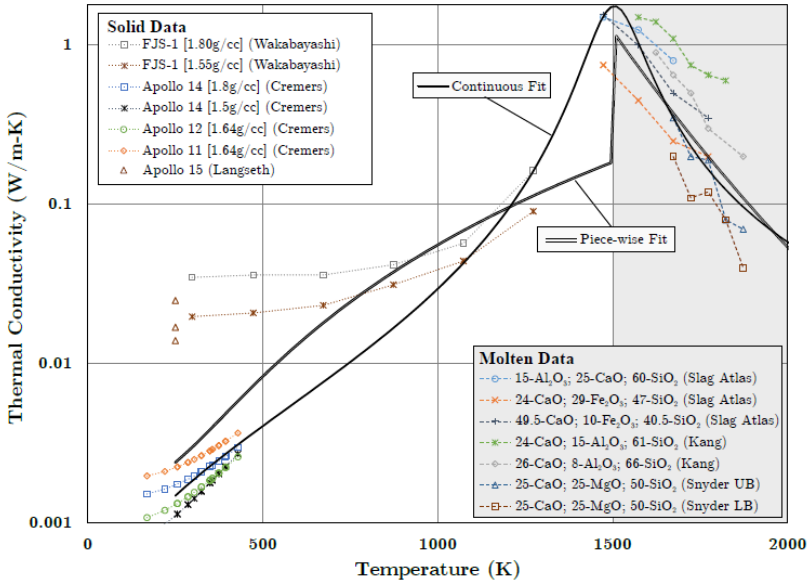

Figure 5. Regolith thermal conductivity (Schreiner et al[2]).

Regolith Specific Heat Capacity

The specific heat of the regolith simulant as a function of temperature (shown in Figure 6) was obtained from published work by Whittington et al.[3] The data curve for LHS-1 was used in the

analysis model because of its similar mineralogy to that of CSM-LHT-1G to be used in the reactor test.

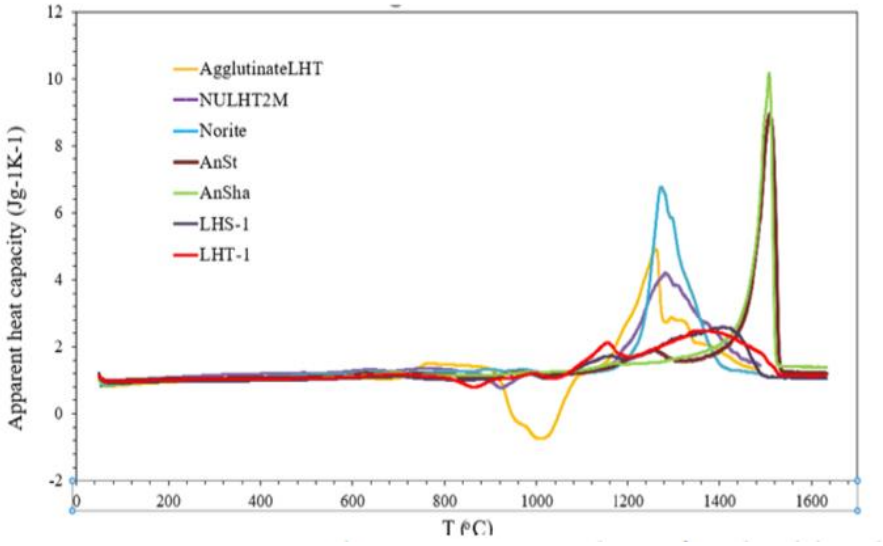

Figure 6. Specific heat capacity of selected simulants (Whittington et al.[3]).

Regolith Density

The density of regolith in its natural granular form depends primarily on the degree of compaction of the soil. It ranges from 1500 to 1775 kg/m^3 for all types of regolith[2]. In the molten state, the mineralogy of the regolith is the dominant factor as illustrated in Figure 7. The data featured for Highland's regolith was used in the model as representative of the CSM-LHT-1G simulant.

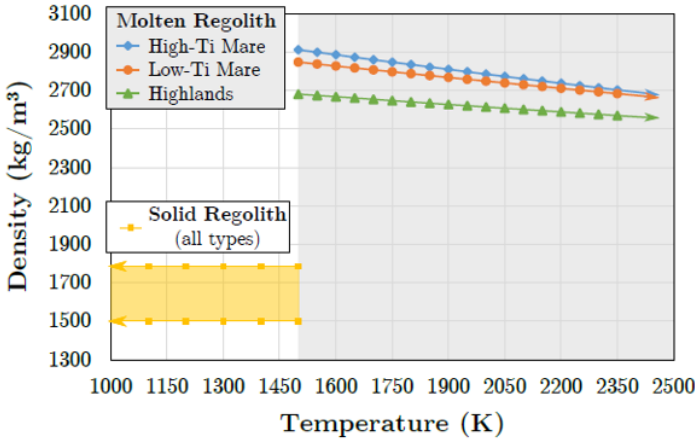

Figure 7. Density of lunar regolith in solid and molten state (Schreiner et al[2]).

Regolith Participating Media Absorption Curve

The radiative heat transfer through molten regolith at high temperatures is dependent on the optical response of the material expressed by the absorption curve obtained from Sibille et al.[4] and Schreiner et al[2] (Figure 8). The absorption length is plotted as a function of wavelength and temperature.

	Gauss 1	Gauss 2	Gauss 3	Gauss 4	Gauss 5
$\mathbf{a}_i$	465	-0.650	163	0.325	1.45
$\mathbf{b}_i$	-3670	200	528	175	150
$\mathbf{c}_i$	5040	4.69	905	4.40	3.54

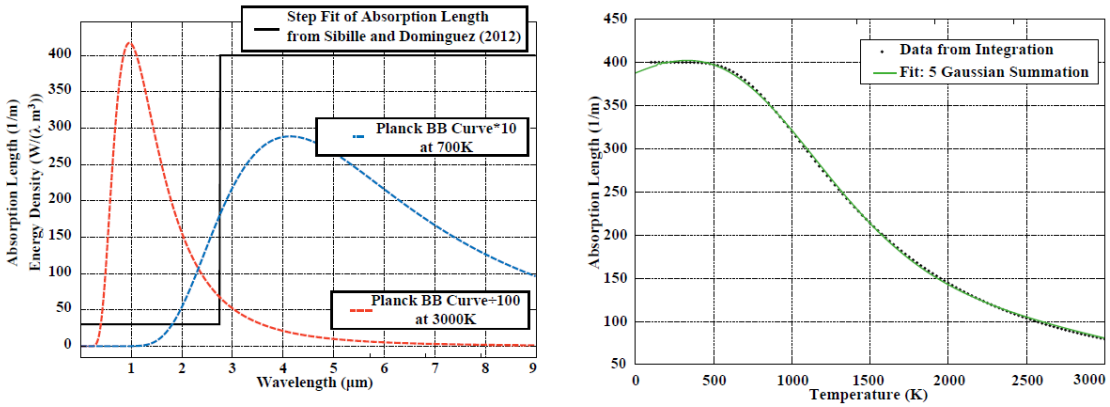

Figure 8. Average Optical absorption plots for granular and molten regolith.

ASSIST Materials Overview

Table 2 lists the materials used for the different components and structures in the ASSIST chamber.

Table 2. Materials selected for ASSIST components.

AISI 304	ASSIST Chamber walls
Brick	ASSIST Chamber Floor
Aluminosilicate Blanket	ASSIST Chamber Floor
Aluminum 5052	Radiation Shield for ASSIST Door
Glass (borosilicate)	ASSIST Windows
Fiberglass	Wire coatings

MODELING AND ANALYSIS

CFD Modeling

The heating phase of the regolith induces the thermal evolution of water from the mineral grains by desorption and dissociation of chemically bound hydroxyl and water molecules in the form of water vapor that dominates the total volatile production during this phase. The modeled water vapor evolution includes two temperature-dependent phases. During the initial heating of the regolith from 20℃ to 500℃, an inlet steam flow rate boundary condition above the regolith is assigned a constant value of 4.78 x 10^{-5} kg/s. After the regolith reaches a temperature of 500℃ the flow rate is linearly decreased to about 10% of the maximum flow rate at the end of the heating phase (17.5 hours) when the regolith temperature at 2 cm from the heating system reaches 1400℃ (Figure 9).

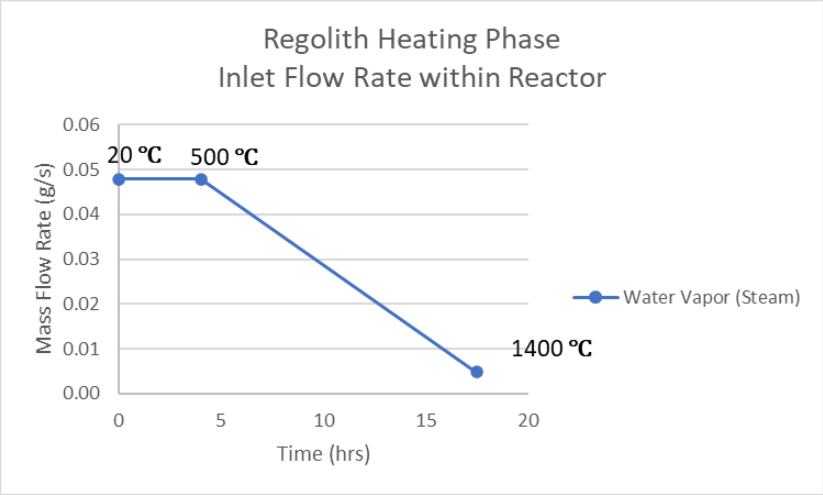

Figure 9. Water vapor flow rate from regolith.

The outlet pressure boundary condition for the water vapor (steam) is increased linearly within the same regolith temperature range to a maximum value (Figure 10). Initially the pressure above the regolith is at vacuum pressure (approx. 1.3x10^{-3} Pa (10^{-5} Torr)). As the heating system heats the regolith water vapor forms and the pressure outlet boundary condition increases linearly to 2.0 psia (13,789.5 Pa) at 17.5 hours when the regolith temperature at 2 cm from the heating system reaches 1400℃.

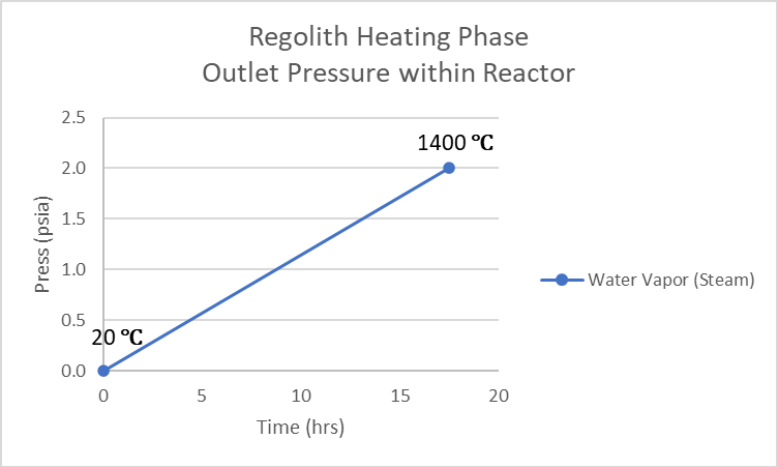

Figure 10. Assigned outlet pressure of water vapor.

During the electrolysis phase, O_2 is assumed to be the only gas produced from the melt with a constant inlet mass flow rate of 6 x 10^{-5} kg/s. The outlet pressure was set to a constant 2.0 psia. The surfaces within the regolith were set to 1600°C.

Fluid Flow Analysis

The water vapor and O_2 fluid analysis was set to laminar flow, and walls had no slip conditions.

$$\frac{\partial \rho}{\partial t} + \nabla \cdot (\rho \boldsymbol{u}) = 0 \tag{1}$$

$$\rho \frac{\partial \boldsymbol{u}}{\partial t} + \rho(\mathbf{u} \cdot \nabla)\mathbf{u} = \nabla \cdot [-p\mathbf{I} + \mathbf{K}] + \mathbf{F} \tag{2}$$

$$\rho C_p \left(\frac{\partial T}{\partial t} + (\mathbf{u} \cdot \nabla)\mathbf{T}\right) = -(\nabla \cdot \mathbf{q}) + \mathbf{K}\!:\mathbf{S} - \frac{T}{\rho}|_p(\frac{\partial P}{\partial t} + (\mathbf{u} \cdot \nabla)\mathbf{p} + \mathbf{Q} \tag{3}$$

Where

ρ is the density (SI unit: kg/m^3)

u is the velocity vector (SI unit: m/s)

p is pressure (SI unit : Pa)

I is the identity matrix (unitless)

K is the viscous stress tensor (SI unit: Pa)

F is the volume force vector (SI unit: N/m^3)

C_p is the specific heat capacity at constant pressure (SI unit: J/(kg·K))

T is the absolute temperature (SI unit: K)

q is the heat flux vector (SI unit: W/m^2)

Q contains the heat sources (SI unit: W/m^3)

S is the strain-rate tensor:

$$\boldsymbol{S} = \frac{\mathbf{1}}{\mathbf{2}}(\boldsymbol{\nabla u} + (\mathbf{\nabla u})^{\boldsymbol{T}}) \tag{4}$$

The operation ":" denotes a contraction between tensors defined by

$$\boldsymbol{a}\mathbf{:}\boldsymbol{b} = \sum_{\boldsymbol{n}} \boldsymbol{a_{nm}} \sum_{\boldsymbol{m}} \boldsymbol{b_{nm}} \tag{5}$$

and sometimes known as the double dot product.

For a Newtonian fluid, which has a linear relationship between stress and strain, Stokes deduced the following expression:

$$\boldsymbol{K} = \mathbf{2}\boldsymbol{\mu S} - \frac{\mathbf{2}}{\mathbf{3}}(\boldsymbol{\nabla} \cdot \boldsymbol{u})\boldsymbol{I} \tag{6}$$

The dynamic viscosity, μ (SI unit: Pa·s), for a Newtonian fluid is allowed to depend on the thermodynamic state but not on the velocity field. The water vapor and O_2 in this analysis were considered Newtonian.

Thermal Modeling

Heat Transfer in Solids

$$\boldsymbol{\rho C_p}(\frac{\boldsymbol{\partial T}}{\boldsymbol{\partial t}} + \boldsymbol{u_{trans}} \cdot \boldsymbol{\nabla T}) + \boldsymbol{\nabla} \cdot (\boldsymbol{q} + \boldsymbol{q_r}) = \boldsymbol{\alpha T}\mathbf{:}\frac{\boldsymbol{dS}}{\boldsymbol{dt}} + \boldsymbol{Q} \tag{7}$$

$$\boldsymbol{q} = -\boldsymbol{k}\boldsymbol{\nabla T} \tag{8}$$

Where

ρ is the density (SI unit: kg/m^3)

C_p is the specific heat capacity at constant stress (SI unit: J/(kg·K))

T is the absolute temperature (SI unit: K)

u_{trans} is the velocity vector of translational motion (SI unit: m/s)

q is the heat flux by conduction (SI unit: W/m^2)

q_r is the heat flux by radiation (SI unit: W/m^2)

α is the coefficient of thermal expansion (SI unit: 1/K)

S is the second Piola-Kirchhoff stress tensor (SI unit: Pa)

Q contains additional heat sources (SI unit: W/m^3)

Heat Transfer in Fluids

$$\boldsymbol{\rho C_p}(\frac{\partial \boldsymbol{T}}{\partial \boldsymbol{T}} + \boldsymbol{u} \cdot \boldsymbol{\nabla T}) + \boldsymbol{\nabla} \cdot (\boldsymbol{q} + \boldsymbol{q_r} = \boldsymbol{\alpha_p T}\left(\frac{\partial \boldsymbol{p}}{\partial \boldsymbol{t}} + \boldsymbol{u} \cdot \boldsymbol{\nabla p}\right) + \boldsymbol{\tau}\colon \boldsymbol{\nabla u} + \boldsymbol{Q} \quad (9)$$

$$\boldsymbol{q} = -\boldsymbol{k}\boldsymbol{\nabla T} \quad (10)$$

$$\boldsymbol{\rho} = \frac{\boldsymbol{pA}}{\boldsymbol{R_s T}}\ \boldsymbol{in\ ideal\ gas\ domain} \quad (11)$$

Where

ρ is the density (SI unit: kg/m^3)

A is the molar mass of the gas (SI unit: g/mol)

C_p is the specific heat capacity at constant pressure (SI unit: J/(kg·K))

T is the absolute temperature (SI unit: K)

u is the velocity vector (SI unit: m/s)

q is the heat flux by conduction (SI unit: W/m^2)

q_r is the heat flux by radiation (SI unit: W/m^2)

p is the pressure (SI unit: Pa)

τ is the viscous stress tensor (SI unit: Pa)

Q contains heat sources other than viscous dissipation (SI unit: W/m^3)

α_p is the coefficient of thermal expansion (SI unit: 1/K):

$$\boldsymbol{\alpha_p} = -\frac{\boldsymbol{1}}{\boldsymbol{\rho}}\frac{\boldsymbol{\partial \rho}}{\boldsymbol{\partial T}} \quad (5)$$

for ideal gases, the thermal expansion coefficient takes the simpler form $\alpha_p = 1/T$

Surface-to-Surface Radiation

The COMSOL Multiphysics model included surface-to-surface radiation using the Ray Shooting method resolution set to 8, tolerance set to 1e-3, maximum number of adaptations set to 3 and a maximum number of reflections set to 1000. The surfaces were set to diffuse gray body except for a highly reflective surface at the back of the ASSIST chamber set as a diffuse mirror. Also, the ASSIST door windows were set as a semitransparent surface with a transmissivity set to 0.8.

$$\boldsymbol{J} = \boldsymbol{\varepsilon e_b}(\boldsymbol{T}) + \boldsymbol{\rho_d G_{ext}} \quad (12)$$

$$\boldsymbol{G} = \boldsymbol{G_m} + \boldsymbol{G_{amb}} + \boldsymbol{G_{ext}} \quad (13)$$

$$\boldsymbol{G_{amb} = F_{amb}\varepsilon_{amb}e_b(T_{amb})} \quad (14)$$

$$\boldsymbol{e_b(T_{amb}) = n^2\sigma T^4} \quad (15)$$

Where

F_{amb} is the view factor of the ambient portion of the field of view

ε is the surface emissivity

ρ_d is the diffuse reflectivity

n is the refractive index

T is the absolute temperature (SI unit: K)

G is the total incoming radiative flux called irradiation (SI unit: K)

J is the total diffuse outgoing radiative flux called radiosity (SI unit: W/m^2)

e_b(T) is the power radiated across all wavelengths and depends on the fourth power of the temperature

σ is the Stefan–Boltzmann constant ($\sigma = 5.67 \times 10^{-8}$ W/m^2 · K^4)

Radiation in Participating Media (Molten Regolith)

The molten regolith medium absorbs a fraction of the incident radiation. The amount of absorbed radiation is κI(Ω), where κ is the absorption coefficient. The absorption coefficient is obtained from Schreiner et al.[2].

$$\boldsymbol{Q_r = \kappa(G - 4\pi I_b(T))} \quad (16)$$

$$\boldsymbol{\nabla \cdot (-D_{P1}\nabla G) = -\kappa(G - 4\pi I_b(T))} \quad (17)$$

$$\boldsymbol{I_b(T) = \frac{n_r^2\sigma T^4}{\pi}} \quad (18)$$

Where

n_r is the refractive index (SI unit: 1)

κ, is the absorption coefficient, (SI unit: 1/m)

T is the temperature (SI unit: K)

For an opaque surface, using gray surface type,

$$\boldsymbol{n \cdot (-D_{P1}\nabla G) = q_{r.net}} \quad (19)$$

where D_{P1} is the P1 diffusion coefficient and ε the surface emissivity.

The P1 approximation is the simplest approximation provided by the method of spherical harmonics method (PN-method). This approximation provides additional accuracy compared to a

Rosseland approximation even if it remains a very simple method. The P1 method relies on the following hypotheses:

- The media is optically thick media: $\tau >> 1$, where τ is the optical thickness defined by the integral of absorption coefficient, κ, along a typical optical path:
$$\tau = \int_0^S \kappa ds \quad (20)$$
- The scattering is linear isotropic.

From a computational point of view this approximation has a limited impact because it introduces only one additional degree of freedom for the incident radiation G (SI unit: W/m^2), which is a scalar quantity and adds a heat source or sink to the temperature equation to account for radiative heat transfer contributions. This method, however, fails to accurately represent cases where the radiative intensity propagation dominates over its diffusivity or where the scattering effects cannot be described by a linear isotropic phase function.

Radiative heat flux is included in addition to conductive heat flux to couple radiation in participating media.

$$\boldsymbol{\rho C_p}\left(\frac{\partial \boldsymbol{T}}{\partial \boldsymbol{T}} + \boldsymbol{u}\cdot\boldsymbol{\nabla T}\right) + \boldsymbol{\nabla}\cdot(\boldsymbol{q}+\boldsymbol{q_r}) = \boldsymbol{\kappa}(\boldsymbol{G} - \boldsymbol{4n\sigma T^4}) + \boldsymbol{\alpha_p T}\left(\frac{\partial \boldsymbol{p}}{\partial \boldsymbol{t}} + \boldsymbol{u}\cdot\boldsymbol{\nabla p}\right) + \boldsymbol{\tau}\colon\boldsymbol{\nabla u} + \boldsymbol{Q} \quad (21)$$

Convective Heat Transfer

$$-\boldsymbol{n}\cdot\boldsymbol{q} = \boldsymbol{q_0} \quad (22)$$

$$\boldsymbol{q_0} = \boldsymbol{h}(\boldsymbol{T_{ext}} - \boldsymbol{T}) \quad (23)$$

Where

q is the conductive heat flux vector (SI unit: W/m^2), $q = -k\nabla T$.

n is the normal vector on the boundary.

q_0 is the inward heat flux (SI unit: W/m^2), normal to the boundary.

T_{ext} is the external fluid temperature (SI unit: K)

T is the temperature at the boundary surface (SI unit: K)

h is the convective heat flux (SI unit: W/m^2)

Water Cooled Walls

The ASSIST chamber has three water-cooled walls for which a heat transfer coefficient of 500 W/m^2-K was selected for the forced flow cooling with water at 20℃ and an external temperature of 20 ℃. An emissivity of 0.3 was selected for both inside and outside ASSIST chamber walls.

ASSIST Chamber Front Door (Natural Convection)

Heat transfer through the external wall of the door is modeled as convective heat flux, with a heat transfer coefficient of 25 W/m^2-K and an external temperature of 20 ℃.

ASSIST Chamber External Floor (Fan Cooled)

Heat transfer through the external wall of the floor is modeled as forced convective heat flux, with a heat transfer coefficient of 100 W/m^2-K and an external temperature of 20 ℃.

Mesh

The modeling employs a user-controlled mesh, with corner refinement. The mesh operation creates an unstructured tetrahedral mesh with 787,188 total elements (Figure 11).

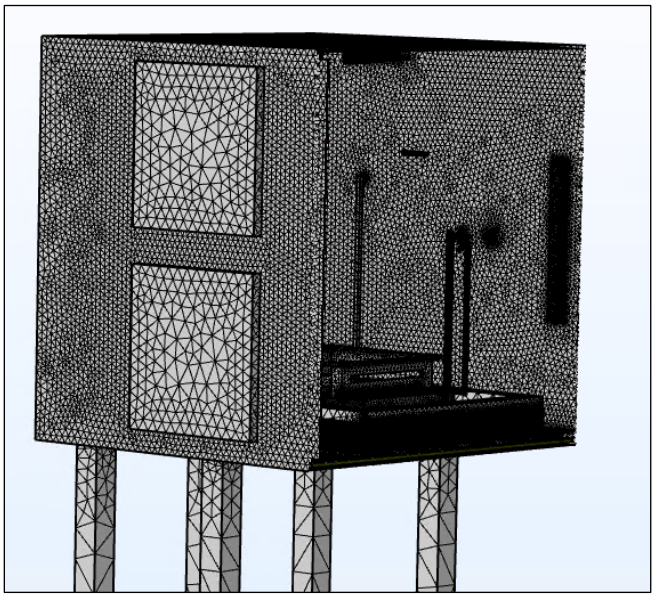

Figure 11. ASSIST chamber mesh.

Solver

The segregated solution approach was used. This attribute makes it possible to split the solution process into sub-steps. Each sub-step uses a damped version of Newton's method.

The iterative linear system solver GMRES (Generalized Minimum RESidual) was used for the fluid variables.

The Time-Dependent Solver used the implicit time-stepping BDF (backward differentiation formula) method for solving ordinary differential equations (ODEs).

RESULTS

The contour temperature plot in Figure 12 shows the temperatures on components above and below the reactor within the ASSIST chamber at the completion of the assumed test duration (37.5 h).

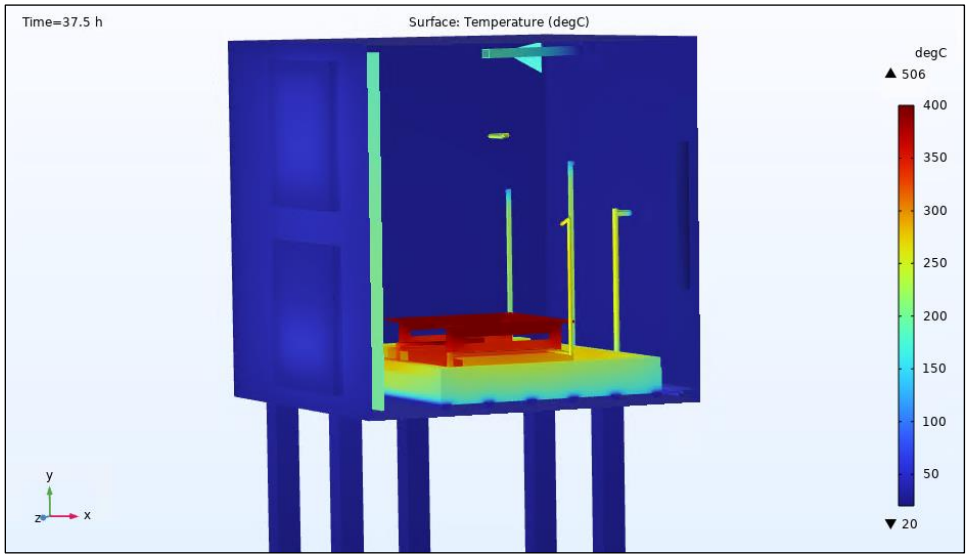

Figure 12. ASSIST chamber internal temperature contour plot.

Figure 13 displays a contour temperature plot for the temperatures on the front door of the ASSIST chamber and the two borosilicate windows. The thermal simulation indicates the maximum window temperatures to be 55°C and the maximum door temperature to be 49°C after 37.5 hours.

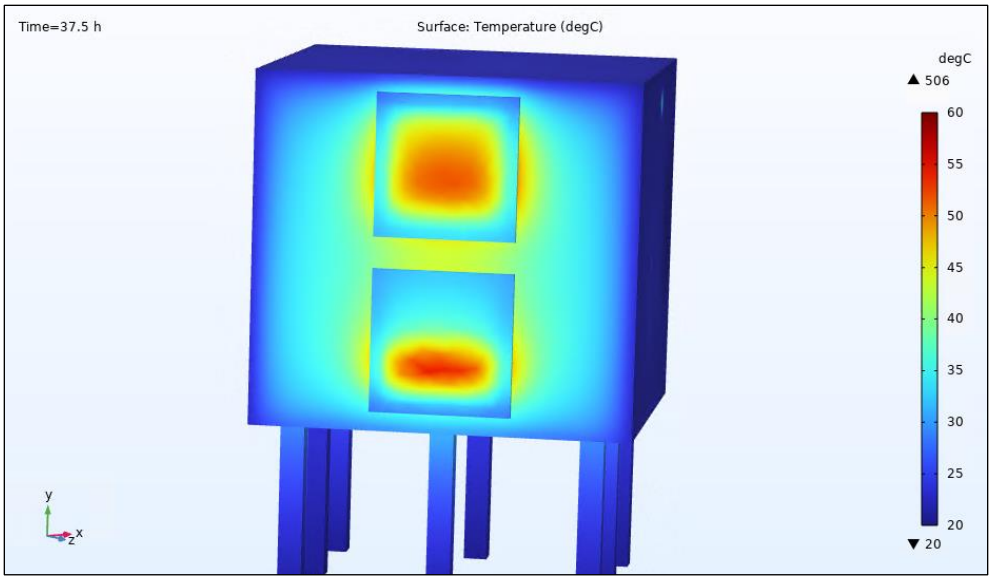

Figure 13. Internal temperature contour plot of ASSIST door elements.

The contour temperature plot **in** Figure 14 shows the temperatures on the aluminum shield protecting the front door of the ASSIST chamber. The two cut outs show the front windows.

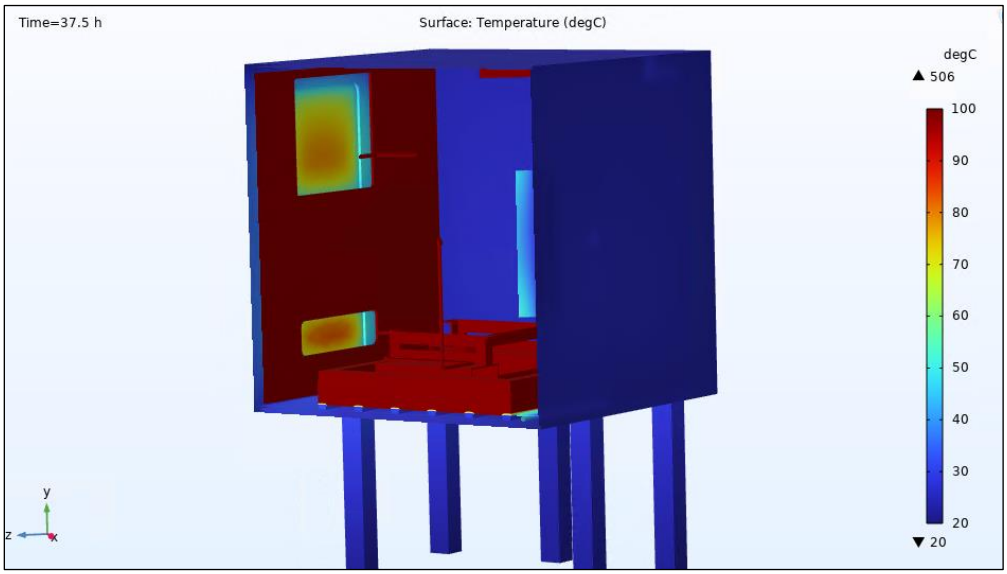

Figure 14. ASSIST chamber internal aluminum shield temperature contour plot.

The graph in Figure 15 shows the temperature history plot during the transient analysis at the heating system surface and in the regolith 2 cm from the heating system surface. The transition of

boundary conditions at the end of the heating phase from 1400℃ to 1600℃ is shown as a step marking the beginning of the electrolysis phase.

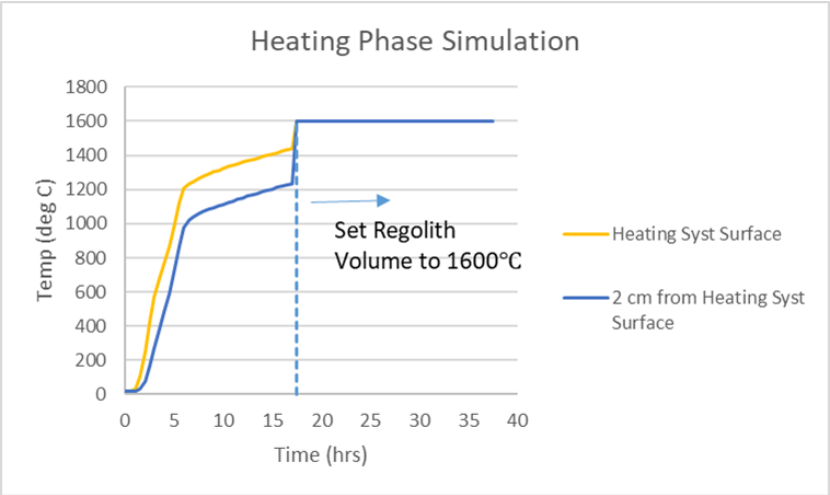

Figure 15. Heating phase to electrolysis phase: Temperature time history plot.

The graph in Figure 16 shows the temperature history plots during the transient analysis at various locations on the ASSIST walls. The three water-cooled ASSIST wall temperatures have a much smaller temperature rise and similar transient temperature profiles compared to the ASSIST floor transient temperatures since the floor is not water cooled.

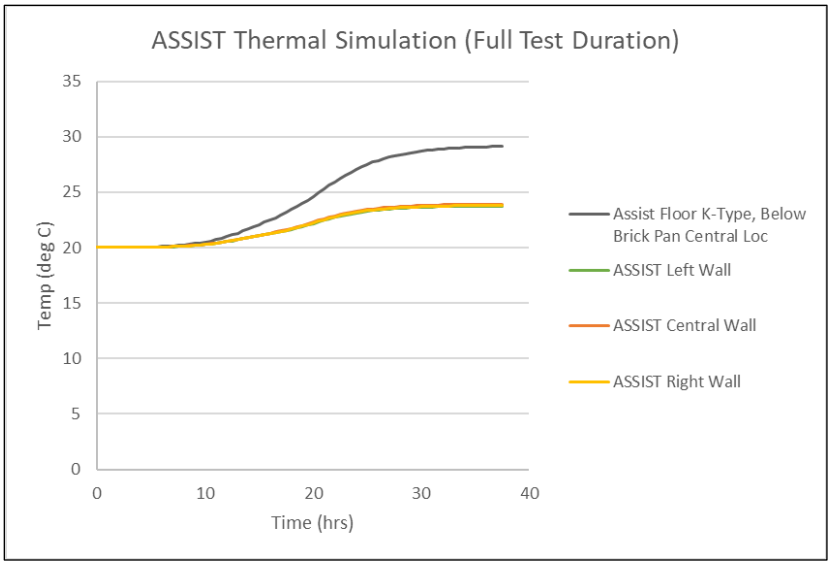

Figure 16. ASSIST chamber wall temperature time history.

The graph in Figure 17 shows the temperature time history plots during the transient analysis at various locations on the reactor.

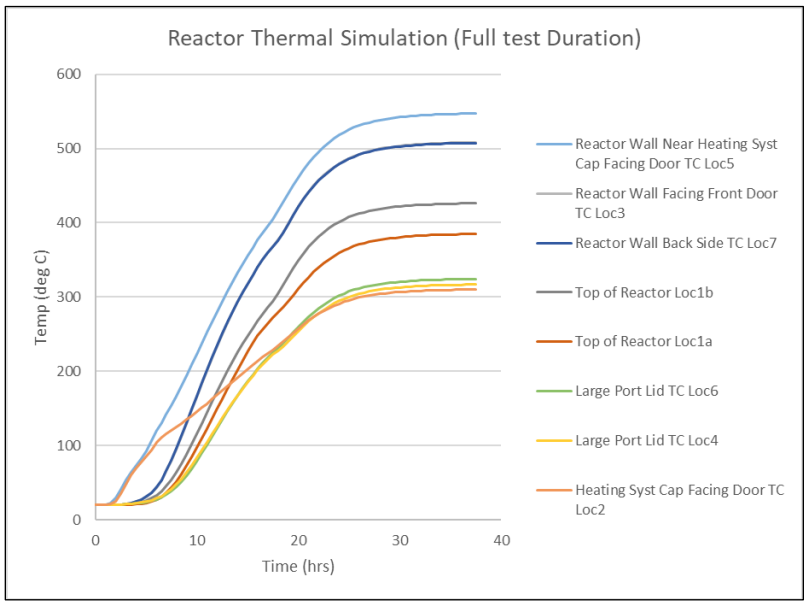

Figure 17. Reactor temperature time history plot.

The graph in Figure 18 shows the temperature time history plot during the transient analysis at various locations of electrical connector and wires in the proximity of the reactor.

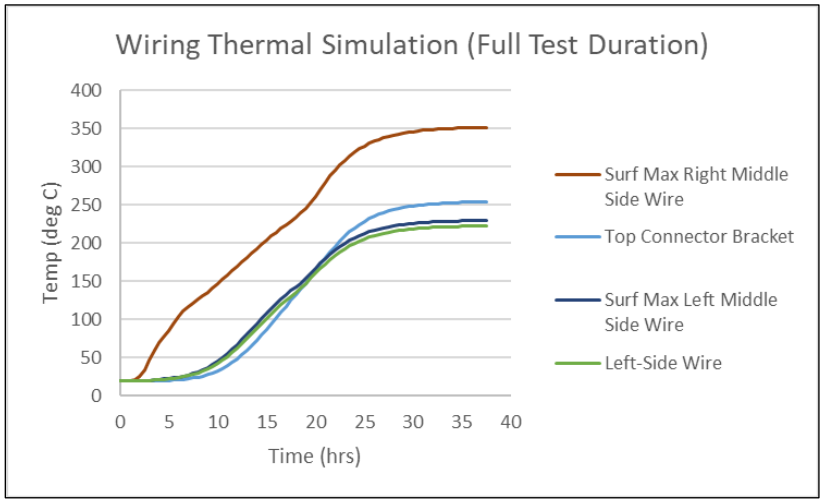

Figure 18. Wiring thermal simulation for full test duration.

Figure 19 displays the dimensions of the regolith height and width along with the regolith temperature 2D contour plot at the end of the heating phase at 17.5 hours when the molten regolith reaches 1400℃ at locations 2 cm from the active heating zone surface. Figure 20 shows a 3D iso-surface plot of the melt domain at the same time mark.

The temperature of the surfaces contacting the melt domain is set at a constant 1600℃ after 17.5 hours to simulate the electrolysis phase. This includes the anode, cathode and any surface of the heating system in contact with the melt area.

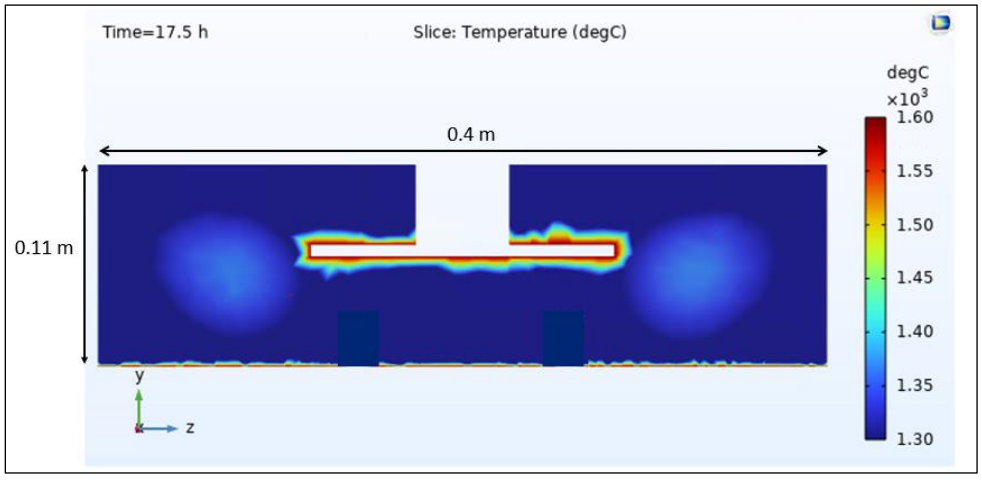

Figure 19. 2D contour temperature plot of the regolith volume at 17.5 hours.

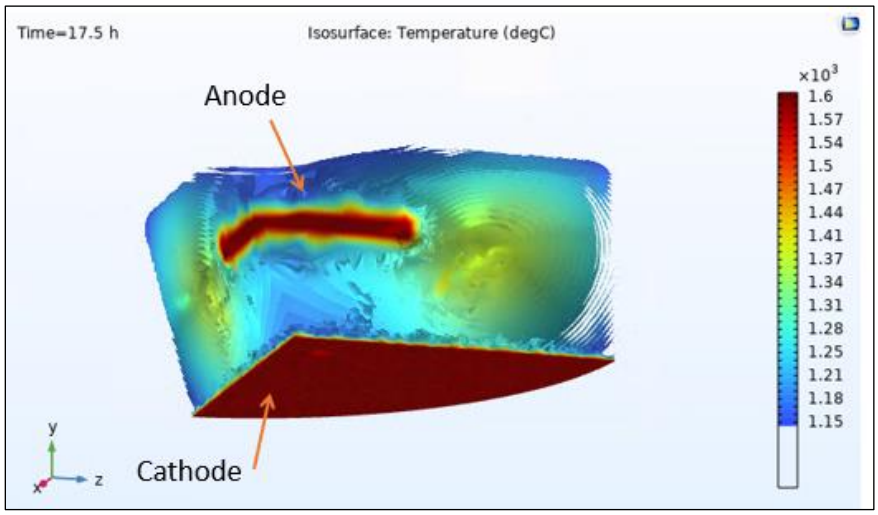

Figure 20. Temperature iso-surface cross-sectional plot of the regolith volume at the end of the heating phase (17.5 hours).

Figure 21 shows the regolith temperature 2D contour plot at 20 hours at which point the melt domain surfaces have been maintained at 1600℃ for 2.5 hours following the transition from the heating phase to the electrolysis phase.

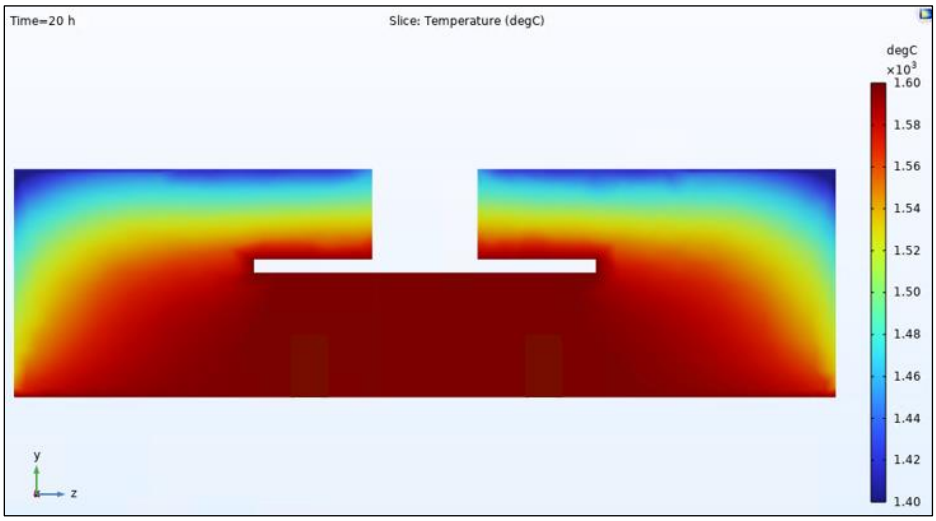

Figure 21. 2D contour temperature plot of the regolith volume at 20 hours.

Figure 22 shows the regolith temperature 2D contour plot at the completion of the electrolysis phase (37.5 hours). The volume of molten regolith between the anode and the cathode remains at the desired operating temperature 1600℃ thus validating the surface boundary conditions.

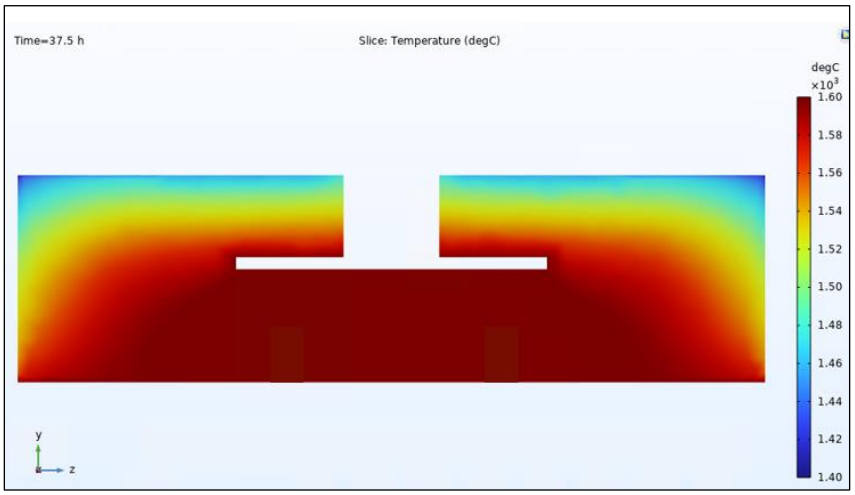

Figure 22. 2D contour temperature plot of the regolith volume at 37.5 hour.

Figure 23 shows an 3D iso-surface cross-sectional plot at 37.5 hours displaying details of the temperature gradient throughout the molten phase with a top surface at a temperature lower by 100℃. The top surface is cooled by the flow of water vapor and O_2 exiting from it.

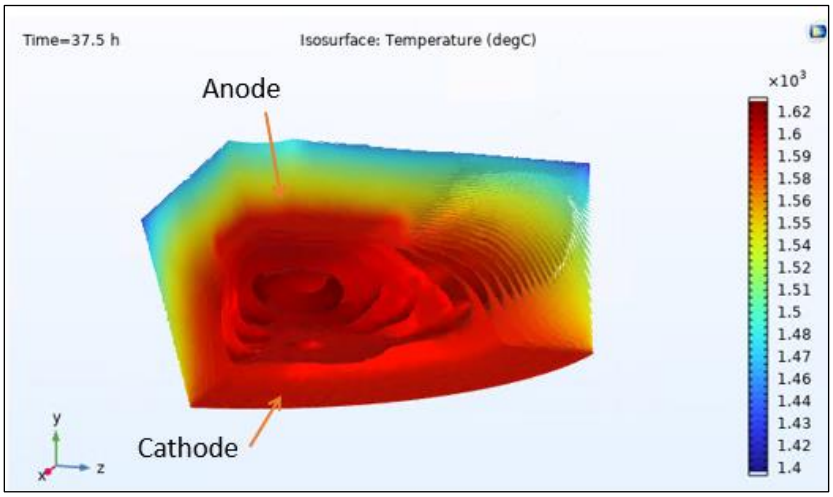

Figure 23. Temperature iso-surface cross-sectional plot of the regolith volume at the end of the electrolysis phase (37.5 hours).

The rate of heat loss associated with water vapor (steam) as a function of time is displayed in Figure 24 during the heating phase (first 17.5 hours). The COMSOL CFD analysis modeled the region above the melt pool and simulated the flow of water vapor. The inlet and outlet temperature were monitored to calculate the rate of heat lost due to the convection of heated water vapor leaving the top of the reactor shown in the graph below. Once the electrolysis begins the fluid domain above the melt pool was updated to O_2. The COMSOL CFD analysis modeled the flow of O_2 similarly to that of steam. The inlet and outlet temperature were monitored to calculate the rate of heat loss due to the convection of heated O_2 leaving the top of the reactor (Figure 24).

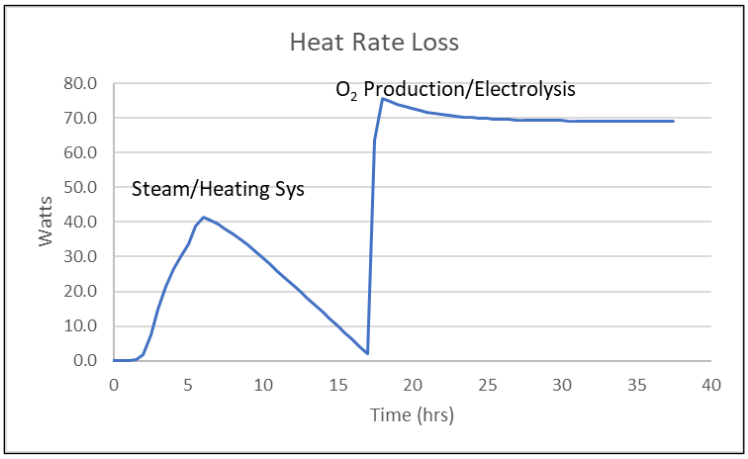

Figure 24. Rate of heat loss due to steam and O_2.

The velocity contours of the O_2 leaving the reactor are displayed in the volume above the melt pool at the end of the test (37.5 hours) in Figure 25.

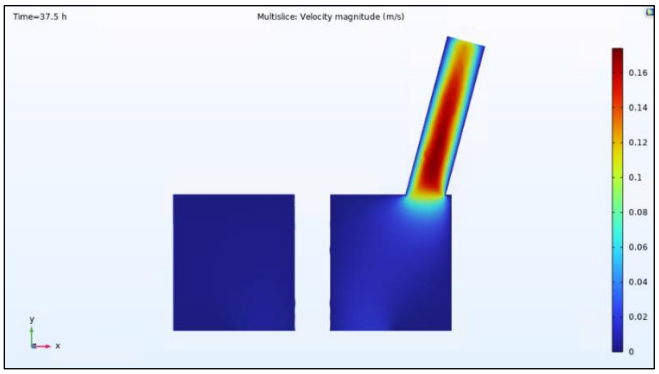

Figure 25. Velocity contour plot of O_2 exiting the reactor.

The contour plot in Figure 26 shows the pressure contours of the O_2 above the melt pool and the outlet channel at the end of the test (37.5 hours).

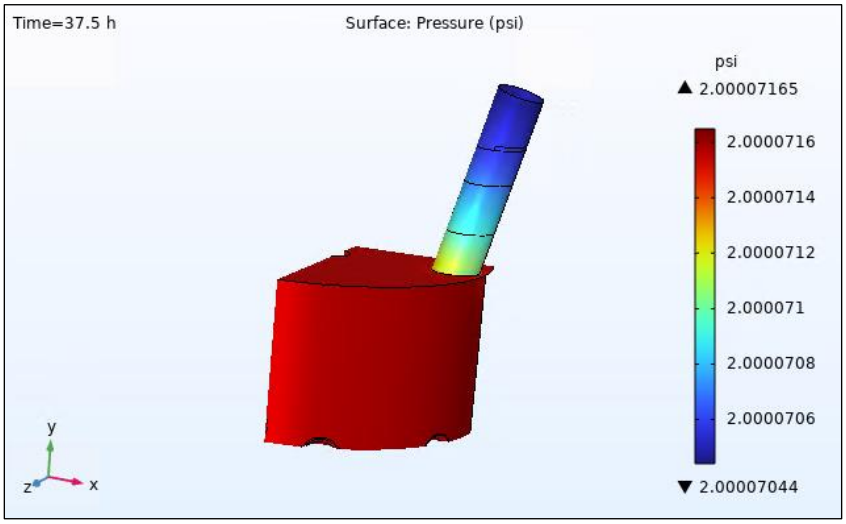

Figure 26. Pressure contour plot of O_2.

The contour plot in Figure 27 shows the temperature contours of the O_2 above the melt pool and through the outlet channel at the end of the test (37.5 hours).

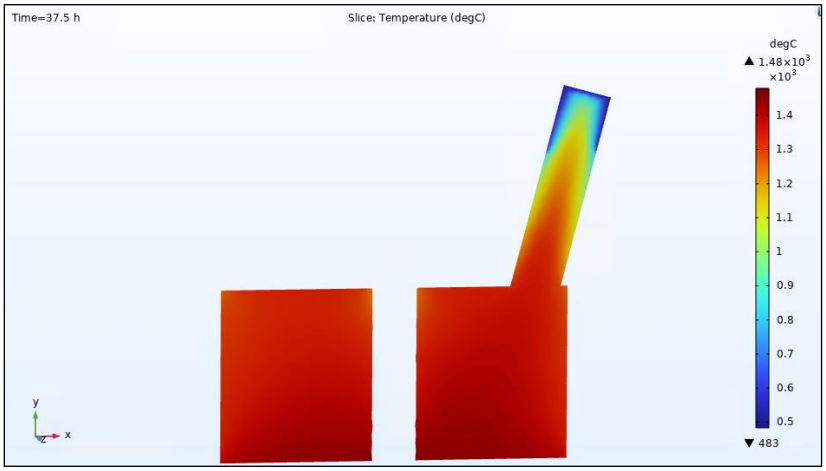

Figure 27. Temperature contour plot of O_2 gas flow.

CONCLUSIONS

A transient thermal/CFD analysis of the reactor and thermal vacuum chamber was created to simulate the thermal behavior of the reactor containing a molten mass of regolith in the ASSIST chamber for different analysis cases. The thermal simulation model was used to characterize both the reactor during two operational phases and the thermal environment of the ASSIST during reactor operations and identify protection options for internal walls as needed to limit temperatures to below 150 ℃ on the internal walls of the ASSIST chamber.

ACKNOWLEDGEMENTS

The authors would like to thank Kennedy Space Center Molten Regolith Electrolysis team for their support of this work and Lunar Resources, Inc. for their assistance with MRE reactor specifics.

REFERENCES

[1] COMSOL Multiphysics, Software Package, Ver. 6.1, COMSOL AB, Stockholm, Sweden, 2022.

[2] Schreiner, S.S., Dominguez, J.A., Sibille, L. and Hoffman, J.A., 2016. Thermophysical property models for lunar regolith. Advances in Space Research, 57(5), pp.1209-1222

[3] Whittington, A.G., Morrison, A.A., Parspapoor, A., Patridge, A., (2023) Thermal and Rheological Properties of lunar Simulants from Ambient to Molten Glass, 54th Lunar and Planetary Science Conference 2023 (LPI Contrib. No. 2806). Available at: https://www.hou.usra.edu/meetings/lpsc2023/pdf/2811.pdf (Accessed: 27 July 2024).

[4] Sibille, L. and Dominguez, J., 2012. Joule-heated molten regolith electrolysis reactor concepts for oxygen and metals production on the Moon and Mars. In 50th AIAA Aerospace Sciences Meeting including the New Horizons Forum and Aerospace Exposition (p. 639).